AMERICAN SCIENTIFIC PUBLISHERS

Advanced Science Letters
Vol. 2, 356–359, 2009

Fabrication and Characterization of Crystalline Cubic Bismuth Zinc Niobate Pyrochlore ($Bi_{1.5}ZnNb_{1.5}O_7$) Nanoparticles Derived by Sol–Gel

Satyendra Singh[1], Amit Kumar Mondal[2], and S. B. Krupanidhi[1,*]

[1]*Materials Research Centre, Indian Institute of Science, Bangalore 560012, India*
[2]*Institute Nanoscience Initiative, Indian Institute of Science, Bangalore 560012, India*

Here, we report the fabrication and characterization of crystalline cubic bismuth zinc niobate pyrochlore, $Bi_{1.5}ZnNb_{1.5}O_7$, (BZN) nanoparticles. A novel sol–gel method is used for the synthesis of air-stable and precipitate-free diol-based sols of BZN which was dried at 150 °C and partially calcined at 350 °C/1 h to decompose organics and bring down the free energy barrier for crystallization. Annealed at 450–700 °C/1 h, BZN powder exhibited nanocrystalline morphology. The average BZN nanoparticle size were about 6, 60 and 85 nm for the samples annealed at 450, 600 and 700 °C/1 h, respectively as observed by transmission electron microscope (TEM). The crystallinity and phase formation of the as synthesized nanoparticles were confirmed by the selected-area electron diffraction (SAED), X-ray diffraction (XRD) and high resolution TEM (HRTEM) analysis. Energy-dispersive X-ray spectroscopy (EDX) analysis demonstrated that stoichiometric $Bi_{1.5}ZnNb_{1.5}O_7$ was formed.

1. INTRODUCTION

Nanostructures such as, nanoparticles, nanocubes, nanorods, nanobelts, nanosheets, nanowires, and nanotubes of various materials, have become one of the most highly pursued research areas because of their fascinating size dependent properties (optical, electronic, magnetic, thermal, mechanical, and chemical), which are distinct from their bulk counterparts and their relevant applications in mesoscopic physics and nanoscale device fabrication.[1–11] Since electroceramic materials are following a similar trend to miniaturization as conventional semiconductors, the synthesis of nanosized oxidic building blocks is moving into the focus of scientific and technological interest. Recently, tunable dielectric materials have attracted considerably attention for the scientific and engineering communities for tunable microwave devices, such as tunable filters, phase shifters, resonators and tunable antennas. For microwave applications, the ideal materials should combine a high tunability with low dielectric loss. Pyrochlore and pyrochlore-related compounds in the Bi_2O_3–ZnO–Nb_2O_5 system exhibit high dielectric constants, relatively low dielectric losses, and compositionally adjustable temperature coefficients of capacitance. These properties, allied to low sintering temperatures (less than 950 °C), make these compounds attractive candidates for capacitor and high-frequency filter applications in multilayer structures co-fired with metal electrodes.[12]

Recently, cubic pyrochlore phase $Bi_{1.5}ZnNb_{1.5}O_7$ have attracted much attention due to their medium permitivity, low-temperature coefficient, and very low dielectric losses ($<10^{-4}$ at 1 MHz).[13–17] In thin film form, the dielectric losses remain low at least up to 20 GHz [17,18] and hence BZN thin films are attractive for microwave tunable application.[18–20] Silva et al.[21] have prepared BZN nanopowder by a urea-modified polymeric precursor method but the main problem in that method was the formation of large agglomerates of clusters of nanoparticles. Present work describes the fabrication of BZN nanoparticles by sol–gel processing without the aid of surface modifications, stabilizer and dispersants.

2. EXPERIMENTAL DETAILS

An air-stable and precipitate-free sol of BZN was synthesized by chemical methods based on the diol route[22] whereas 1,3-propanediol, [$HO(CH_2)_3OH$] and glacial acetic acid [CH_3COOH] where used as solvents, while bismuth acetate [$Bi(CH_3CO_2)_3$, 99.99% purity, Aldrich], zinc acetate [$Zn(CH_3CO_2)_2$, 99.99% purity, Aldrich] and niobium ethoxide, [$Nb(OC_2H_5)_5$, 99.95% purity, Aldrich] were used as the precursors. BZN precursor solution was prepared whereby bismuth acetate was dissolved in 1,3-propanediol and glacial acetic acid

*Author to whom correspondence should be addressed.

 1936-6612/2009/2/356/004 doi:10.1166/asl.2009.1042

with continuous stirrer at 100 °C till the complete dissolution of bismuth acetate and then zinc acetate was added to that solution. After complete dissolution of these acetates, niobium ethoxide was added drop by drop to the solution and stirrer at 80 °C for 30 min and the solution was cool to room temperature. The pH value of the final solution was adjusted to 6 by adjusting 1,3-propanediol and glacial acetic acid. The solution, that is usually called BZN precursor solution, was colorless and transparent. The BZN precursor solution was heated on a hot plate whose temperature was increased gradually to 150 °C until a thick sol was formed. The sol, in turn, was heated in a furnace at 200 °C until a porous material was obtained as a result of complete removal of solvents. The dried gel was ground to fine powder and partially calcined at 350 °C/1 h in the alumina crucible to decompose organics and bring down the free energy barrier for crystallization. This powder was annealed in the furnace at 450, 600 and 700 °C for 1 h. Finally, yellowish white BZN powder was obtained. This reaction starts with the nucleophilic addition of negatively charged HO-groups on the positively charged metal atom in the transition state. The positively charged proton is then transferred toward an alkoxy group and the positively charged protonated ROH ligand is finally removed. The chemical reactivity of metal alkoxides toward hydrolysis and condensation mainly depends on the positive charge of the metal atom and its ability to increase its coordination number.[23] A proposed reaction scheme according to Livage et al.[24] is shown in Figure 1.

The fine particles were suspended in acetone medium and dropped on the carbon coated grid. The morphology, selected-area electron diffraction (SAED), structure and composition of the resulting BZN nanoparticles were studied on a transmission electron microscope (TEM, Tecnai F30) equipped with EDX and operated at an accelerating voltage 200 kV. X-ray powder diffraction data were collected on a Philips X'pert pro diffractometer with a copper source.

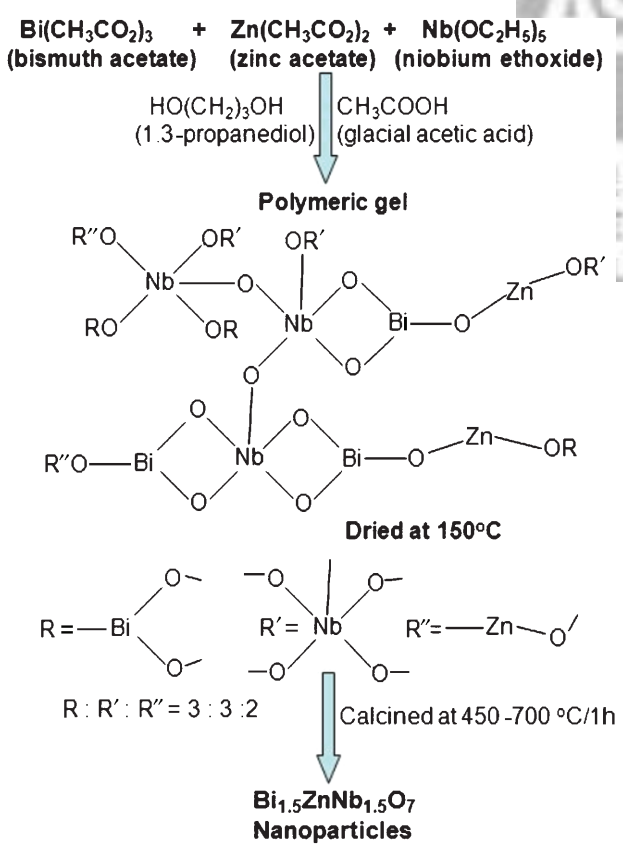

Fig. 1. Proposed reaction scheme for fabrication of BZN nanoparticles.

3. RESULTS AND DISCUSSION

Three different BZN samples were investigated inside the TEM. Figures 2(a–c) show TEM images of BZN precursor powder annealed at 450, 600 and 700 °C for 1 h respectively. The images clearly revel that the particle size distribution were about 3–8 nm, 50–65 nm and 80–95 nm in the BZN precursor powder after annealing at 450, 600 and 700 °C respectively. It was observed that no large agglomerates of clusters of nanoparticles were formed in our method. However, BZN nanopowder prepared by a urea-modified polymeric precursor method[21] contained large hard agglomerates of clusters of nanoparticles. As expected, increasing the annealing temperature caused the increase in particle size in the samples, as illustrated in Figures 2(a–c). Figures 2(d–f) shows the selected area electron diffraction (SAED) patterns corresponding to the BZN precursor powder annealed at 450, 600 and 700 °C respectively. These SAED patterns clearly show that crystallinity increases with annealing temperature. We have indexed SAED pattern

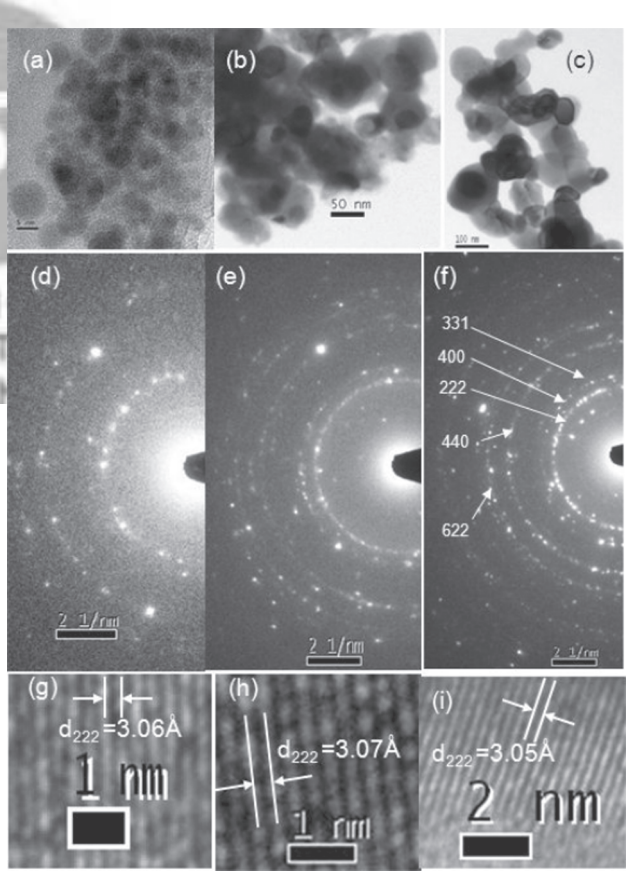

Fig. 2. TEM images: BZN nanoparticles calcined at (a) 450 °C, (b) 600 °C and (c) 700 °C for 1 h, respectively; SAED patterns of BZN nanoparticles calcined at (d) 450 °C, (e) 600 °C and (f) 700 °C for 1 h, respectively; HRTEM images of BZN nanoparticles calcined at (g) 450 °C, (h) 600 °C and (i) 700 °C for 1 h, respectively.

corresponding to the BZN powder annealed at 700 °C shown in Figure 2(f). Circular rings in this SAED pattern corresponding to the (222), (400), (331), (440) and (622) planes reflections of the cubic pyrochlore phase of bismuth zinc niobate. The lattice spacings were calculated from the diameter of the bright circular rings observed in the electron diffraction pattern and compared the data available in the literature. The lattice d-spacings d_{222}, d_{400}, d_{331}, d_{440} and d_{622} were 3.07, 2.65, 2.44, 1.87 and 1.61 Å respectively, which are in good agreement with open literature (JCPDS, # 00-054-0971). Figures 2(g–i) show the high-resolution transmission electron microscope (HRTEM) images taken on the isolated nanoparticles present in the BZN precursor powder annealed at 450, 600 and 700 °C, respectively, which gives further insight into the details of the microstructure of the BZN nanoparticles. The distance between the parallel fringes is about 3.06 Å, corresponding to the well-recognized lattice d-spacing of (222) atomic planes, which agrees well with the values, calculated from the SAED pattern. The particles were oriented along the [222]. The HRTEM pattern of large particle or agglomerate show the same structure and orientation as the isolated particle and thus provides evidence that the larger structures indeed consist of assembled BZN nanoparticles.

The TEM results were further verified by X-ray diffraction analysis. XRD results of BZN precursor gel annealed at 450, 600 and 700 °C/1 h are shown in the Figures 3(a–c). It was observed that the phase transformation of the BZN precursor gel to cubic pyrochlore phase was started as early as 450 °C, as can be seen in the Figure 3(a). It may be observed that the numbers of counts from the most intense XRD peak (222) were around 450, 1100 and 1700 for the samples annealed at 450, 600 and 700 °C, respectively, which indicate that with increasing annealing temperature the degree of crystallinity increases in the samples, as shown in Figure 3. The XRD pattern of BZN powder exhibited broad peaks indicative of fine size of BZN particles and the peak broadening decreases with increasing annealing temperature. The average crystallite size was found about 30, 60 and 90 nm for the samples annealed at 450, 600 and 700 °C, respectively which were calculated from Scherrer's formula by indexing (222) peak as follows;

$$T = 0.9\lambda/\beta\cos\theta_B$$

where T is the average particle size in angstroms, β is the width of the peak at half the peak height in radians, λ (=1.5406 Å) is the wavelength in angstroms, and θ_B is the Bragg angle in degrees. The average crystallite size as calculated by the Scherrer's formula well matched with the particle size observed by TEM for the samples annealed at 600 and 700 °C. Scherrer's formula, however, could not verify the TEM result for the sample annealed at 450 °C/1 h.

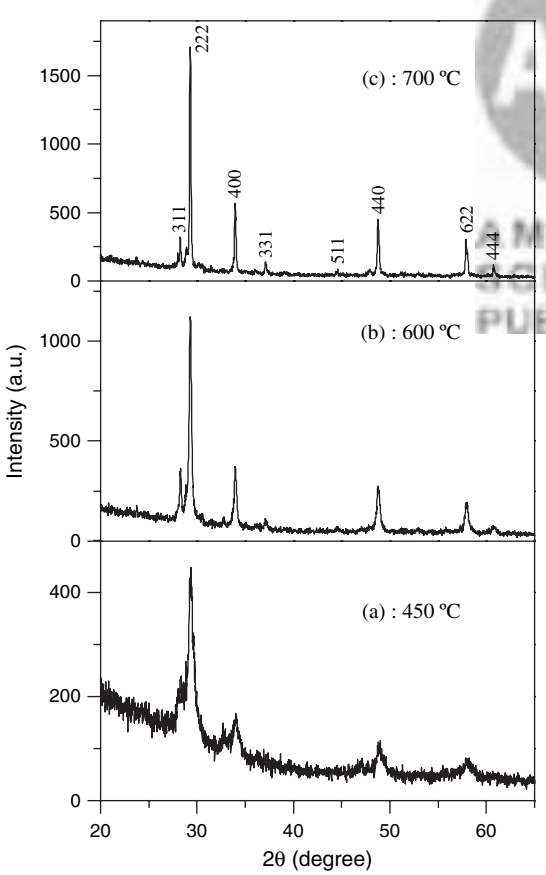

Fig. 3. XRD pattern of BZN nanoparticles calcined at (a) 450 °C, (b) 600 °C and (c) 700 °C for 1 h, respectively.

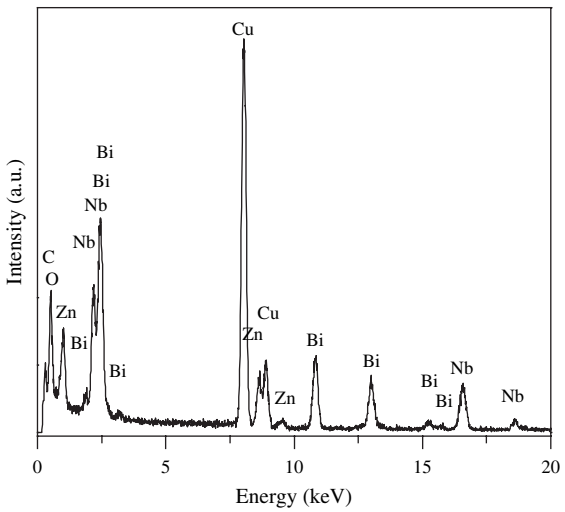

Fig. 4. EDX spectrum from BZN nanoparticles calcined at 700 °C for 1 h.

In order to determine the chemical composition of as prepared BZN nanoparticles, EDX experiments were performed on individual nanoparticle by the TEM. Only the freestanding isolated nanoparticles were selected in the experiments to avoid effects due to supporting carbon film and other nanoparticles. Figure 4 shows the typical EDX spectra from a nanoparticle present in the sample annealed at 700 °C for 1 h. The presence of Bi, Zn, Nb and O peaks in the spectra indicate that these nanoparticles are made of Bi, Zn, Nb and O and the average atomic ratio of Bi:Zn:Nb:O are 0.158:0.093:0.161:0.593 which is very close to the desired composition $Bi_{1.5}ZnNb_{1.5}O_7$. The presence of some Cu and C peaks may be attributed to the Cu and carbon coating on TEM grids.

4. CONCLUSIONS

To summarize, crystalline BZN nanoparticles were fabricated by a novel sol–gel method based on diol-based solution. The crystallization of the cubic BZN pyrochlore phase was detected at

a temperature as low as 450 °C. XRD and TEM analysis confirmed the nanocrystalline nature of BZN particles. The crystallinity and the particle size of the as synthesized BZN powders were increased with rising annealing temperature. This technique is also applicable for the synthesis of other complex oxides for large scale production. The nanoparticles can be used for making high quality ceramics and composites because ceramic materials are following a similar trend to miniaturization as conventional semiconductors so the synthesis of nanosized oxidic building blocks is moving into the focus of scientific and technological interest.

References and Notes

1. Y. Xia, P. Yang, Y. Sun, Y. Wu, B. Mayers, B. Gates, Y. Yin, F. Kim, and H. Yan, *Adv. Mater.* 15, 353 **(2003)**.
2. G. R. Patzke, F. Krumeich, and R. Nesper, *Angew. Chem., Int. Ed.* 41, 2446 **(2002)**.
3. C. M. Lieber, *MRS Bull.* 28, 486 **(2003)**.
4. B. L. Cushing, V. L. Kolesnichenko, and C. J. O. Connor, *Chem. Rev.* 104, 3893 **(2004)**.
5. C. N. R. Rao and A. K. Cheetham, *J. Mater. Chem.* 11, 2887 **(2001)**.
6. C. N. R. Rao and M. Nath, *Dalton Trans.* 1 **(2003)**.
7. J. C. Hulteen and C. R. Martin, *J. Mater. Chem.* 7, 1075 **(1997)**.
8. G. Schmid, *J. Mater. Chem.* 12, 1231 **(2002)**.
9. Z. W. Pan, Z. R. Dai, and Z. L. Wang, *Science* 291, 1947 **(2001)**.
10. Z. L. Wang, *J. Mater. Chem.* 15, 1021 **(2005)**.
11. X. S. Fang, C. H. Ye, L. D. Zhang, and T. Xie, *Adv. Mater.* 17, 1661 **(2005)**.
12. I. Levin, T. G. Amos, and J. C. Nino, *J. Solid State Chem.* 168, 69 **(2002)**.
13. R. L. Thayer, C. A. Randall, and S. Trolier-McKinsky, *J. Appl. Phys.* 94, 1941 **(2003)**.
14. H. Wang, R. Elsebrock, T. Schneller, R. Waser, and X. Yao, *Solid State Commun.* 132, 481 **(2004)**.
15. H. J. Youn, T. Sogabe, C. A. Randall, T. R. Shrout, and M. Lanagan, *J. Am. Ceram. Soc.* 84, 2557 **(2001)**.
16. C. Ang, Z. Yu, H. J. Youn, C. A. Randall, A. S. Bhalla, L. E. Cross, J. Nino, and M. Lanagan, *Appl. Phys. Lett.* 80, 4807 **(2002)**.
17. J. W. Lu and S. Stemmer, *Appl. Phys. Lett.* 83, 2411 **(2003)**.
18. J. Park, J. W. Lu, D. S. Boesch, S. Stemmer, and R. A. York, *IEEE MWC Lett.* 16, 264 **(2006)**.
19. J. Park, J. W. Lu, D. S. Boesch, S. Stemmer, and R. A. York, *J. Appl. Phys.* 97, 084110 **(2005)**.
20. A. K. Tagantsev, J. W. Lu, and S. Stemmer, *Appl. Phys. Lett.* 86, 032901 **(2005)**.
21. S. A. da Silva and S. M. Zanetti, *Mater. Chem. Phys.* 93, 521 **(2005)**.
22. M. L. Calzada, M. Alguero, J. Ricote, A. Santos, and L. Pardo, *J. Sol–Gel Sci. Techn.* 42, 331 **(2007)**.
23. J. Livage, C. Sanchez, and F. Babonneau, Chem Adv Mater, edited by L. V. Iterrante and M. J. Hampde-Smith, Wiley-VCH, New York **(1998)**, Chap. 9, p. 389.
24. J. Livage, M. Henry, and C. Sanchez, *Prog. Solid State Chem.* 18, 259 **(1988)**.

Received: 11 January 2009. Accepted: 12 January 2009.